

EcoLoc: Toward Universal Location Sensing by Encounter-Based Collaborative Indoor Localization

Hsinchung Chen
Department of Electrical Engineering
and Computer Science, University of
California, Irvine
hsinchuc@uci.edu

Yi Lin Chen
Department of Computer Science,
National Tsing Hua University,
Hsinchu, Taiwan
lin781219@gmail.com

Chia Hsun Wu
Department of Computer Science,
National Tsing Hua University,
Hsinchu, Taiwan
k8142311@gmail.com

Mohammad Abdullah Al
Faruque
Department of Electrical Engineering
and Computer Science, University of
California, Irvine
alfaruqu@uci.edu

Pai H. Chou
Department of Electrical Engineering
and Computer Science, University of
California, Irvine
phchou@uci.edu

ABSTRACT

Indoor localization techniques proposed to date have assumed costly resources in terms of computation, power, or sensing modality for many wearable end-devices in the Internet of Things (IoT). To make localization a universal feature for IoT devices, we propose EcoLoc, an indoor localization system using collaborative version of Conditional Random Fields (CCRF) integrated with our encounter model to generate the most probable locations. We have implemented EcoLoc on the Android tablet and the Broadcom WICED Sense IoT platform with a lower-power MCU, miniature inertial sensors, and Bluetooth Low-Energy (BLE) radio. Experimental results show that while operating without the aid of beacons, compared to the non-collaborative CRF, EcoLoc can shorten the convergence distance by up to 40% on tablet, and up to 50% on the WICED-Sense while incurring an extra current consumption of 15 mA.

CCS CONCEPTS

•Computer systems organization →Sensor networks;

KEYWORDS

IoT, collaborative indoor localization

1 INTRODUCTION

The knowledge of location is fundamental to enabling devices in the Internet of Things (IoT) to behave in an intelligent way. While outdoor localization is relatively well understood based on a combination of GPS and cellular tower triangulation, indoor localization remains a challenge especially for many IoT devices [15]. Existing

indoor localization techniques can be categorized into reference-based vs. self-referential, respectively [23].

Reference-based techniques use geometric relationship with landmarks to estimate the location by measuring some signal generated or reflected by the landmark such as proximity sensing[9], triangulation [7], and fingerprinting [5]. However, these reference-based localization techniques rely on measuring reference signals, but they can suffer from interference in the physical environment even if the target is not moving. *Self-referential* localization techniques measure the device's own displacement relative to its initial position to determine its current location. They are also generally called dead reckoning, and they consist of a sensing part and a computation part. Sensors used in dead reckoning can be inertial sensors, pedometers, or odometers. In this work, we consider inertial sensors, which usually consist of accelerometers, gyroscopes, and possibly magnetometers. One advantage is that all sensors are small, low-power, inexpensive, and self-contained to track the trajectory independent of landmarks. The computation part estimates the location based on the sensor data. Mathematical techniques proposed to date include the Kalman Filter (KF), Hidden Markov Models (HMMs), and Particle Filters (PF). KF is widely used for not only noise removal but also to estimate the location over time [4, 18]. HMMs [14, 17] and PFs [12, 19] are based on the Bayesian probability model to predict the most probable location. However, these models tend to be computationally intensive for many wearable IoT devices such as the Broadcom WICED Sense tag.

This work represents a major step toward enabling location sensing universally by all mobile IoT devices, not just those higher-end ones equipped with costly sensors and processors in terms of size and power consumption. We exploit BLE for proximity sensing with very low power consumption. The main novelty with our work is that upon encounter, the IoT devices exchange their trajectories to enable fast detection of their respective locations on the map, without relying on centralized servers and even in the absence of beacons or landmarks. The reduced computational complexity is enabled by our use of collaborative conditional random fields.

Fig. 1 shows the architecture of EcoLoc. The trajectory generated from sensors and the shared trajectories from the encounter events are merged by our CCRF to estimate the location by running our

Permission to make digital or hard copies of all or part of this work for personal or classroom use is granted without fee provided that copies are not made or distributed for profit or commercial advantage and that copies bear this notice and the full citation on the first page. Copyrights for components of this work owned by others than ACM must be honored. Abstracting with credit is permitted. To copy otherwise, or republish, to post on servers or to redistribute to lists, requires prior specific permission and/or a fee. Request permissions from permissions@acm.org.

IoT'17, Pittsburgh, PA, USA

© 2017 ACM. ISBN 978-1-4503-4966-6/17/04...\$15.00

DOI: <http://dx.doi.org/10.1145/3054977.3055000>

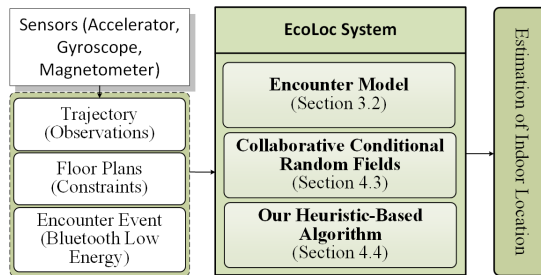


Figure 1: System Architecture of EcoLoc

real-time tracking algorithm with the floor plans constraints. We evaluate our algorithm on Broadcom WICED Sense IoT platforms [3] and Android Nexus 9 tablet.

2 RELATED WORK

Pedestrian dead reckoning (PDR) is a special version of DR that tracks displacement in terms of steps taken by a walking person. Inertial sensors and magnetometer can be used to generate the step count and heading direction, respectively, for estimating displacement. UPTIME [1] proposes pedestrian models to describe the step behavior for optimization of accuracy on smartphone. Furthermore, the fingerprint techniques using WiFi signal [13] can help improve the accuracy of PDR. However, PDR can still have the error accumulation problem due to sensor drift and sensor noise [2]. The error keeps accumulating in the new estimated result since it is based on the previous estimation without correction mechanisms in DR. To overcome this problem, some mathematical techniques have been proposed on top of the PDR to improve the accuracy.

Kalman Filter (KF) is one of the popular techniques for estimating the location while cleaning up sensor data at the same time. LIDAR [18] use the distance sensor to detect the wall on corridors to correct the heading of the pedestrian path. The RSSI of received wireless signals such as WiFi [10] is also leveraged to measure the distance between the target devices and the deployed beacons to correct the error. However, KF cannot provide sufficiently accurate result since it requires high accuracy in the estimated or measured data and is limited to fully utilizing the constraints from the floor plan. *Particle Filter* (PF) is another way for location estimation that is more accurate than KF [20], though at a higher computation cost. PF represents possible locations of the target using particles, a set of random samples that capture the probability of the location as weights. The particles are spread on the locations where we are interested in to estimate location. The main problem of PF is the high computation cost for small mobile IoT devices to maintain the weights associated with the particles for sufficient area coverage. *Conditional random field* (CRF) is considered as an affordable solution for devices with lower computation capability [22]. In our work, EcoLoc integrates the encounter events with CRF to enhance its robustness for indoor localization. In addition, researchers have also proposed techniques that use shared information to enhance localization. The location can be estimated through the information exchanged between known location reference nodes like deployed beacons or other devices [21]. The centralized design that use servers to coordinate devices have also been proposed to estimate

the location of devices systematically [8]. However, these techniques involve a third party to manage and process the information for IoT devices and suffer from the constraints of flexibility and real-time response [16].

3 DATA AND SENSING COMPONENTS

EcoLoc relies on inertial sensors and PDR to generate the trajectories which describe the step behavior of pedestrians. In EcoLoc, the BLE RF is used to sense the proximity between users and define the encounter events to enable the sharing of trajectories as well as detecting beacons.

3.1 Pedestrian Dead Reckoning

EcoLoc utilizes PDR to generate the user trajectories which contain the information of user movement, including step detection, heading orientation, and step length. We adopt the *peak-and-valley* detection method [11] to monitor pedestrian activities. We first define the acceleration change threshold and the time window. If the difference between the maximum and minimum acceleration within the time window is larger than the threshold, a step event is triggered. Meanwhile, the estimation of step length relies on the accelerometer and is influenced by individual factors such as step frequency, walking speed, etc. Since the step-length estimation is outside the scope of this work, we assume the step length is fixed without loss of generality, and a better step-length estimator can be plugged in to improve the accuracy of this work.

The heading orientation can be estimated by the product of gravity and magnetic vector provided by the accelerometer and magnetometer, respectively. In addition, the angular speed provided by gyroscope can also be used to calculate the rotated angle by multiplying the sensor output with the time interval. Considering the accelerometer and magnetometer suffer from the sensor noise, the low-pass filter is applied that the short time variance is eliminated and take the more accurate data over long time period. In contrast, the heading orientation estimated from gyroscope in short time period is more accurate so that the high-pass filter is applied to get the angle change in short time period. Therefore, the noise interference on those inertial sensors can be removed and more accurate data is provided by fusing the sensor data.

3.2 Encounter Model

This work exploits encounter events among multiple devices to enhance the efficiency of indoor localization by enabling sharing of trajectories. EcoLoc utilizes the pairing process to implement the proximity feature based on Bluetooth 4.1, in which the BLE stack supports simultaneously advertising and scanning. During the pairing process, a device, which acts as a scanner, periodically scans the advertising packets sent from other BLE devices, which act as advertisers. The scanner can estimate the distance between itself and the advertiser based on the RSSI. The encounter event is triggered if the packets from advertisers are scanned in certain range. However, due to the use of omnidirectional antenna in most BLE-based systems, it is difficult to determine the direction. Thus, in our system design, the encounter event happens only if the distance between scanner and advertiser is within the step length.

$$\log_{10} D = \frac{A - \text{RSSI}[dbm]}{10n} \quad (1)$$

Eq. (1) is used to measure the distance between two devices. The value of distance is set as the step length, which is the maximum distance between encountered users, and then the RSSI is measured to find the proximity threshold, the minimum RSSI value that two nodes can measure from the received packets within a step length.

We extend the proximity sensing with trajectory exchange for the purpose of enabling collaborative localization. BLE allows data to be piggy-backed onto its advertising payload. This way, it is unnecessary to send the trajectory data in a separate transaction or to go through a connection procedure. However, due to the limited size of the payload, a node sends only a portion of its trajectory instead of the entirety. The original size of the orientation data is 32 bits floating point format. To represent the trajectory in a compact format, we assume that the subject takes one step at a time and can move in only one of eight possible directions (i.e., in 45° increments). This enables us to encode the state transition using only 3 bits using only about 1/10 the original trajectory size. This translates into about 42 steps of trajectory in BLE 4.0 and 4.1, and BLE 4.2 increases the payload size by nearly an order of magnitude.

4 COLLABORATIVE INDOOR LOCALIZATION

In EcoLoc, we utilize CRF to manage the trajectories and propose a real-time algorithm to estimate the location of users.

4.1 Conditional Random Field

CRF can be represented by various feature functions [22] accompanied by weight λ_i formulated as:

$$p(\vec{S}|\vec{Z}) \propto \prod_{j=1}^n \exp\left(\sum_{i=1}^m (\lambda_i f_i(s_{j-1}, s_j, \vec{Z}, j))\right) \quad (2)$$

where j denotes the position in the observation sequence and m is the number of feature functions.

CRF is capable of realizing the probability of state transition by defining complex features such that CRF can take context into account in training and testing phase to enhance the accuracy of estimation. The feature functions f_i represent the constraints provided by the collected observations such as floor map or trajectory. In EcoLoc, CRF consists of feature functions that describe the possibility of location transition by using the corresponding observation. The step detection decides if the CRF estimation is enabled. The heading orientation is used as observation, Z_t^θ , to define our feature function. We assume the heading orientation is a log-normally distributed random variable so that probability density of the log-normal distribution is leveraged to formulate our feature function as follows:

$$f_1 = \ln\left(\frac{1}{\sqrt{2\pi\sigma_\theta^2}}\right) - \frac{(Z_t^\theta - \theta(S_{t-1}, S_t))^2}{2\sigma_\theta^2} \quad (3)$$

where σ_θ^2 is the heading variance of observations Z_t^θ and $\theta(S_{t-1}, S_t)$ is the heading orientation between the last state S_{t-1} and the state S_t that we estimate for the current step.

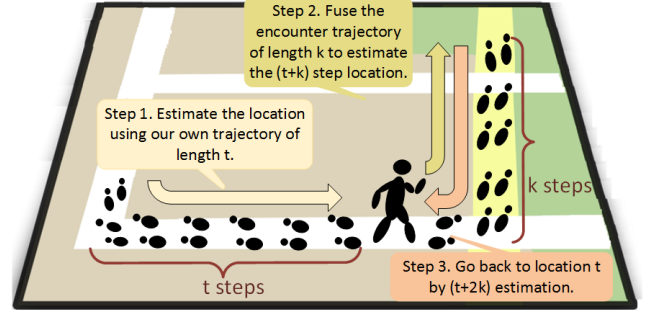


Figure 2: Collaborative Conditional Random Fields

The second feature function is formulated using the RSSI observation. It is optional and is considered only when the beacon signal is available in the indoor environment. Similar to our first feature function, we use the RSSI observation to calculate the distance, Z_t^d , between the user and the beacon B_i to formulate the feature function as follows:

$$f_2 = \ln\left(\frac{1}{\sqrt{2\pi\sigma_d^2}}\right) - \frac{(Z_t^d - D(B_i, S_t))^2}{2\sigma_d^2} \quad (4)$$

where the σ_d^2 is the distance variance of the observations Z_t^d and $D(B_i, S_t)$ is the distance between the beacon and the estimated state.

4.2 Collaborative Conditional Random Field

Our CCRF merges the shared trajectory with our own trajectory to improve the convergence distance of localization.

Our CCRF is illustrated in Fig. 2. It extends the current trajectory with the acquired trajectory from the encounter events. Suppose the length of the acquired trajectory is k steps and our trajectory is t steps, the merged trajectory may not be used to estimate the current location since the estimated location is at step $(t+k)$ instead of at step t . Therefore, our CCRF reverses the acquired trajectory and estimate the location at step $(t+2k)$. The CCRF can be formulated as follows:

$$p(\vec{S}|\vec{Z}) \propto \prod_{j=1}^{t+2k} \exp\left(\sum_{i=1}^m (\lambda_i f_i(s_{j-1}, s_j, \vec{Z}, j))\right) \quad (5)$$

4.3 Our Real-Time Tracking Algorithm

Algorithm 1 shows our real-time tracking algorithm based on Viterbi's [6]. It provides real-time update for IoT devices without estimating from scratch.

At every step, each state will get a score that represents the probability of walking to it from other possible states. Given the observation \vec{z} at step j , the score of s_x transferred from state s_y is calculated through the following equations:

$$\text{score}(s_x, j) = \text{score}(s_y, j-1) \times \Psi_j(s_x | s_y, \vec{z}) \quad (6)$$

$$\Psi_j(s_x | s_y, \vec{z}) = \exp\left(\sum_{i=1}^m (\lambda_i f_i(s_y, s_x, \vec{z}, j))\right) \quad (7)$$

Algorithm 1: Real-time tracking algorithm

Input: The length of output T , observation \vec{Z} , state \vec{S}
Output: The most likely hidden states sequences \vec{X}

- 1 Function HeuristicRealtime (T, \vec{Z}, \vec{S})
- 2 **begin**
- 3 // Calculate the score
- 4 **foreach** $s_x \in \vec{S}$ **do**
- 5 $score[s_x, j] \leftarrow \max_{y \in Valid} (score[s_y, j-1] \times \Psi_j(s_x | s_y, \vec{Z}))$;
 // Estimate the score of states at step j
- 6 $path[s_x, j] \leftarrow \arg \max_{y \in Valid} (score[s_y, j-1] \times \Psi_j(s_x | s_y, \vec{Z}))$; // Store
 the path of states at step j
- 7 $max_state \leftarrow \arg \max_{s_i} score[s_i, T]$; // Find the highest score of
 state at step T
- 8 **for** $i = 0; i < T; i++$ **do**
- 9 $X_i \leftarrow path[max_state, i]$; // Output the path
- 10 **return** X ;

Suppose there are possible states $S = \{s_0, s_1, \dots, s_n\}$ and the length of observation is T . The sequence of the highest score at each step is the trajectory we want. Compared to the exhaustive Viterbi search, the time complexity of our tracking algorithm is $O(|S|^2T)$ instead of $O(|S|^T)$. Furthermore, because only eight states per transition are possible, the time complexity per step is optimized to $O(|S| \times 8) = O(|S|)$.

Our algorithm works as follows. First, each state is assigned a score, which is the highest score among eight calculated results, by using the observation and the score of neighbor states at the previous step (Lines 3-5). The current location is then determined as the state with the highest score (Line 6) and the trajectory is generated as well (Line 8).

5 EXPERIMENTAL VALIDATION

To show the applicability of our proposed technique to a wide range of hardware, we implemented our proposed technique on two platforms: a tablet and a sensor tag. The tablet we use is the Nexus 9, which contains inertial sensors (accelerometer, gyroscope, and magnetometer) as most tablets do and runs Android 6 Marshmallow OS with Bluetooth 4.1 (dual-mode) support. On the lower end, we use the Broadcom WICED Sense Bluetooth Smart Sensor Tag [3] to validate that EcoLoc is applicable for resource-limited IoT devices.

Several evaluation points in Fig. 3 are decided on the floor plan, and the untrained participants can choose any route they like to reach the evaluation points. The tablet-based devices are tested in two different places, but the sensor tags are tested only with the smaller floor plan due to the buffer limitation on physical memory for storing the map information. We also implemented a number of previous techniques for the purpose of comparison with our proposed CCRF. Table 1 shows the technologies used in the experiments.

6 EVALUATION

We evaluate convergence distance, accuracy and algorithm overhead of EcoLoc with other implemented techniques. The experimental results demonstrate the improvement from the collaborative conditional random field.

	Definition
CRF	Ordinary Conditional Random Fields
PF	Particle Filter
CCRF	Encounter-Based Collaborative Conditional Random Fields
CPF	Encounter-Based Collaborative Particle Filter

Table 1: The Acronyms of Implemented Techniques For Evaluation

6.1 Convergence Distance

The *convergence distance* we present here is the displacement required in the estimation to provide a location within a 5-meter radius from the ground truth. A short convergence distance means EcoLoc can operate either without beacons or can operate well while requiring much lower density of deployed beacons.

Fig. 4 shows the convergence distance is significantly shortened by up to 50% compared to the non-encounter CRF in first three evaluation points. This is because the indoor space is limited and the evaluation points we put are closer to the middle of hallway. The two participants walk from either end of the corridor to reach the evaluation points. The convergence distance measured from the rest of two evaluation points did not get improved significantly because of the small indoor space such that the shorter distance is enough to estimate location. We show the convergence distance can benefit from the trajectories exchanged upon encounter and the applicability of EcoLoc on the IoT devices.

The experimental results on the tablet conducted on the 1st and 5th floor of the campus Building are shown in Fig. 5. We compare the results of implemented techniques listed in Table 1. The convergence distances on 5th floor of all four localization techniques are less than 50 meters, which are all shorter than the results on 1st floor, because the trajectory on the 5th floor are more constrained by the floor plan by a turn in the corner. In addition, both CRF and CCRF have shorter convergence distances than PF and CPF do. This is because CRF captures the constraints and is able to provide the most probable location immediately based on the pre-built states; in contrast, PF iteratively generates the new particles to explore the possible locations. In summary, the CRF-based systems need shorter convergence distance than the PF-based systems. Meanwhile, the encounter mechanism significantly help CRF-based localization to reduce the convergence distance.

6.2 Accuracy

We quantify accuracy by measuring how close to the ground truth location each technique can estimate. Our experiments are conducted in different indoor environments with multiple participants to evaluate the accuracy of CRF-based and PF-based localization.

The results we provided for IoT device are shown in Fig. 6. The results provided by CCRF and CRF are close, where the error difference is within one step length. The accuracy of CCRF is sometimes worse than CRF, primarily due to the noisy sensor data. The complex computation is required to filter the noise out of sensor data for DR. However, the error cannot be removed by the exchanged trajectories. In addition, the RSSI from the encounter may be unstable, which makes it difficult to estimate the actual distance accurately. Another source of error is the assumption of constant step length,

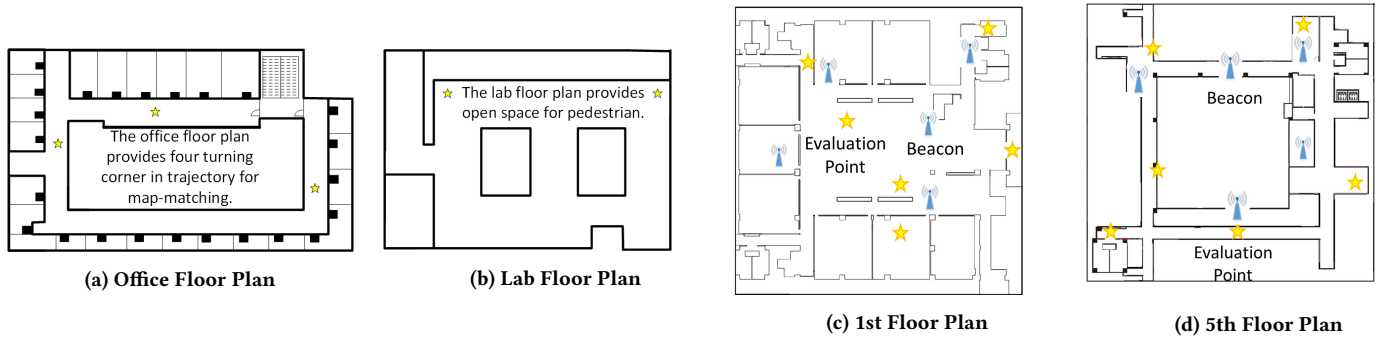


Figure 3: Floor Plans for Our Experiments.

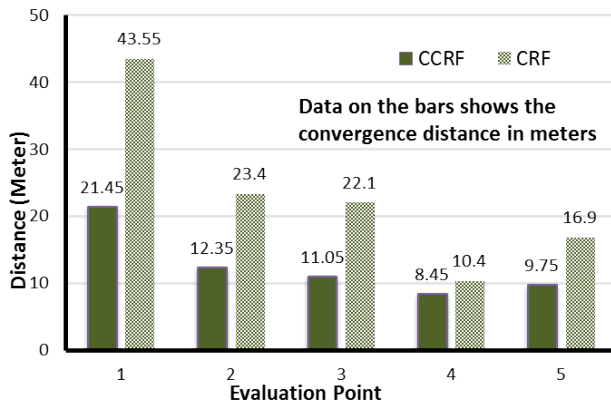


Figure 4: The Comparison of Convergence Distance for WICED-Sense among Five Evaluation Points

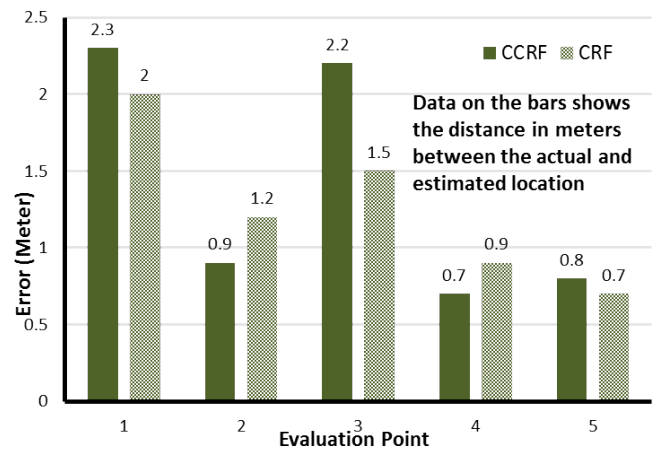


Figure 6: The Comparison of Accuracy for WICED-Sense among Five Evaluation Points.

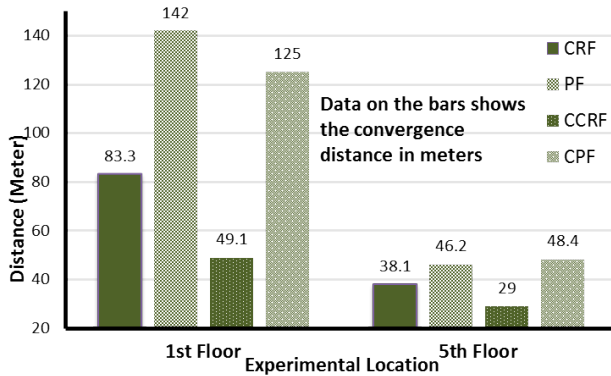


Figure 5: The Comparison of Average Convergence Distance for Tablet on 1st and 5th Floor

but in reality the step length is not constant and can vary among participants.

Fig. 7 compares the average accuracy of these localization techniques on the tablet on the 1st and 5th floor of the campus Building. Overall, the CCRF and CRF can provide the same accurate results. The CRF-based systems are also more accurate than the PF-based systems since the map is preprocessed and divided into several states which provide extra constraints for CRF-based systems.

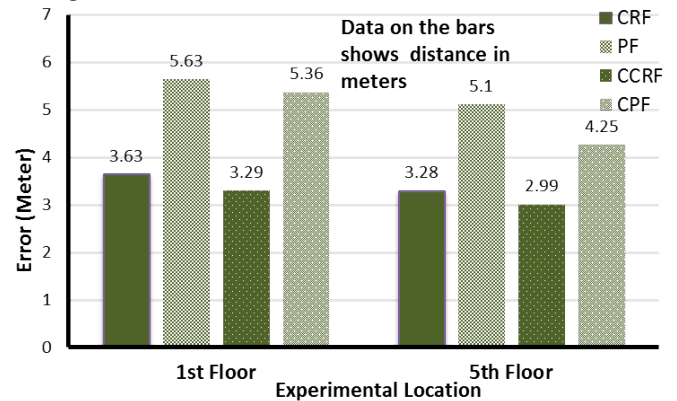


Figure 7: The Comparison of Average Accuracy for Tablet on 1st and 5th Floor without Beacon

6.3 Algorithm Overhead

The overhead is evaluated by measuring the power consumption of our implementation since the APIs for timing measurement are not open source and we are unable to hook up system software. Fig. 8 provides the power consumption comparison of enabling and disabling the encounter event feature. Once the system becomes

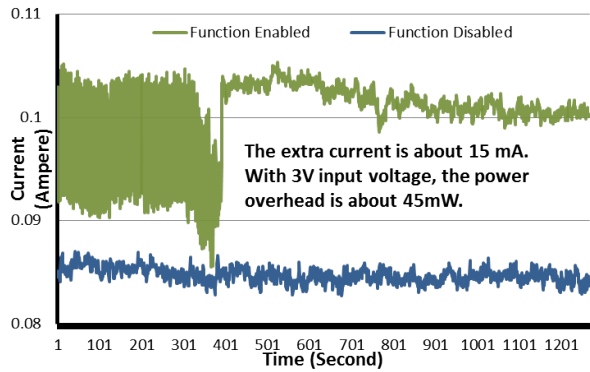


Figure 8: Overhead of Power Consumption for WICED-Sense.

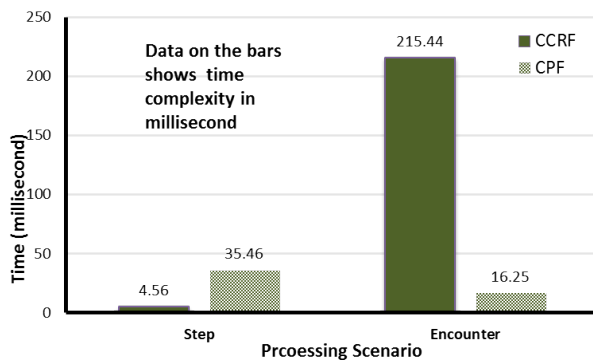


Figure 9: Time Complexity between CCRF and CPF

stable, the difference of current is about 15mA. With 3V input voltage, the extra power consumption is about 45mW.

We observe in the first 400 seconds, the power consumption is caused by the pairing behavior (scanning and advertising). In the last half part, the power overhead comes from the sensor data processing, trajectories exchange, and CCRF trajectories fusion. Note that we put the devices together for a longer period of time to get the precise power data. That is why we can see the device keep high power consuming for such a long time. In our normal operation, the operation period is far fewer than this testing period.

We compare the time complexity of CRF-based system and CPF system running on the tablet. The CPF requires 35.36 ms for the processing in each steps, while the CCRF only spends 4.56 ms. Fig. 9 shows that the execution time when the encounter events occur. Although the CPF can execute the process within 20 ms, which is much lower than CCRF (215.44 ms), it sacrifices the accuracy and convergence distance that we evaluate in the previous sections to acquire the lower time complexity.

7 CONCLUSIONS

To make location knowledge a universal right of all IoT devices, we propose EcoLoc, which requires only low-end processing capabilities and low-power inertial sensors. It exploits sharing of trajectories between devices upon encounter as a way to estimate the location on the map while requiring up to 50% shorter convergence distance than previous techniques. The computation effort is also reduced significantly, thanks to the use of our CCRF model.

The use of BLE makes it practical because it uses the existing RF interface for not only communication but also proximity sensing and encounter exchange. The overhead we measured on IoT device in terms of current consumption is 15 mA.

REFERENCES

- [1] Moustafa Alzantot and Moustafa Youssef. 2012. UPTIME: Ubiquitous pedestrian tracking using mobile phones. In *IEEE Wireless Communications and Networking Conference, (WCNC'12)*. 3204–3209.
- [2] Haitao Bao and Wai-Choong Wong. 2013. An Indoor Dead-Reckoning Algorithm with Map Matching. In *International Wireless Communications and Mobile Computing Conference, (IWCMC'13)*. 1534–1539.
- [3] Broadcom. 2015. WICED Sense Bluetooth Smart Sensor Tag / Experience Kit. <https://www.broadcom.com/products/wireless-connectivity/bluetooth/wiced-sense>. (2015).
- [4] Zhenghua Chen, Han Zou, Hao Jiang, Qingchang Zhu, Yeng Chai Soh, and Lihua Xie. 2014. Fusion of WiFi, Smartphone Sensors and Landmarks Using the Kalman Filter for Indoor Localization. *Sensors* 15, 1 (2014), 715–732.
- [5] R. Faragher and R. Harle. 2014. An Analysis of the Accuracy of Bluetooth Low Energy for Indoor Positioning Applications. In *International Technical Meeting of The Satellite Division of the Institute of Navigation, (ION GNSS+ 2014)*. 201–210.
- [6] G. David Forney. 1973. The Viterbi Algorithm. *Proc. IEEE* 61, 3 (1973), 268–278.
- [7] Christian Gentner and Thomas Jost. 2013. Indoor positioning using time difference of arrival between multipath components. In *International Conference on Indoor Positioning and Indoor Navigation, (IPIN'13)*. 1–10.
- [8] Junghyun Jun, Yu Gu, Long Cheng, Banghui Lu, Jun Sun, Ting Zhu, and Jianwei Niu. 2013. Social-Loc: improving indoor localization with social sensing. In *ACM Conference on Embedded Networked Sensor Systems, (SenSys'13)*. 1–14.
- [9] Swarun Kumar, Stephanie Gil, Dina Katabi, and Daniela Rus. 2014. Indoor localization system using visible light communication. In *International Conference on Mobile Computing and Networking, (MobiCom '14)*. 484–494.
- [10] H. Leppäkoski, J. Collin, and J. Takala. 2015. Pedestrian Navigation Based on Inertial Sensors, Indoor Map, and WLAN Signals. In *IEEE International Conference on Acoustics, Speech and Signal Processing, (ICASSP'12)*. 1569–1572.
- [11] Robert W. Levi and Thomas Judd. 1996. Dead reckoning navigational system using accelerometer to measure foot impacts. (December 1996).
- [12] Fan Li, Chunshui Zhao, Guanzhong Ding, Jian Gong, Chenxing Liu, and Feng Zhao. 2012. A reliable and accurate indoor localization method using phone inertial sensors. In *ACM Conference on Ubiquitous Computing, (UbiComp'12)*. 421–430.
- [13] Kai Lin, Wenjian Wang, Yuanguo Bi, Meikang Qiu, and Mohammad Mehdi Hassan. 2015. Human localization based on inertial sensors and fingerprint in industrial internet of things. *Computer Networks* 15, 1 (2015), 715–732.
- [14] Jingbin Liu, Ruizhi Chen, Yuwei Chen, Ling Pei, and Liang Chen. 2012. iParking: An Intelligent Indoor Location-Based Smartphone Parking Service. *Sensors* 12, 11 (2012), 14612–14629.
- [15] Davide Macagnano, Giuseppe Destino, and Giuseppe Abreu. 2014. Indoor positioning: A key enabling technology for IoT applications. In *IEEE World Forum on Internet of Things, (WF-IoT'14)*. 117–118.
- [16] John-Olof Nilsson, Dave Zachariah, Isaac Skog, and Peter Händel. 2013. Cooperative localization by dual foot-mounted inertial sensors and inter-agent ranging. *EURASIP Journal on Advances in Signal Processing* 2013, 164 (2013).
- [17] Kwanghyo Park, Hyejeong Shin, and Hojung Cha. 2013. Smartphone-based pedestrian tracking in indoor corridor environments. *Personal and Ubiquitous Computing* 17, 2 (2013), 359–370.
- [18] Duy Duong Pham and Young Soo Suh. 2016. Pedestrian Navigation Using Foot-Mounted Inertial Sensor and LIDAR. *Sensors* 16, 1 (2016), 120–126.
- [19] Jiuchao Qian, Jiabin Ma, Rendong Ying, Peilin Liu, and Ling Pei. 2013. An Improved Indoor Localization Method Using Smartphone Inertial Sensors. In *International Conference on Indoor Positioning and Indoor Navigation, (IPIN'13)*. 1–7.
- [20] Anshul Rai, Krishna Kant Chintalapudi, Venkata N. Padmanabhan, and Rijurekha Sen. 2012. Zee: Zero-Effort Crowdsourcing for Indoor Localization. In *International Conference on Mobile Computing and Networking, (MobiCom'12)*. 293–304.
- [21] Reza Monir Vaghefi, Mohammad Reza Gholami, R. Michael Buehrer, and Erik G. Ström. 2013. Cooperative received signal strength-based sensor localization with unknown transmit powers. *IEEE Transactions on Signal Processing, (SP'13)* 61, 6 (2013), 1389–1403.
- [22] Zhuoling Xiao, Hongkai Wen, Andrew Markham, and Niki Trigoni. 2014. Lightweight map matching for indoor localisation using conditional random fields. In *Information Processing in Sensor Networks, (IPSN'14)*. 131–142.
- [23] Lingling Zhu, Aolei Yang, Dingbing Wu, and Li Liu. 2014. Survey of Indoor Positioning Technologies and Systems. *Life System Modeling and Simulation* 461 (2014), 400–409.